Article:
Ji, J, Sun, W, Wang, W et al. (2 more authors) (2014) The effect of mechanical loading on osteogenesis of human dental pulp stromal cells in a novel in vitro model. Cell and Tissue Research, 358 (1). 123 - 133. ISSN 0302-766X

https://doi.org/10.1007/s00441-014-1907-8

The effect of mechanical loading on osteogenesis of human dental pulp stromal cells in a novel in vitro model

Jun Ji[1,2,3], Weibin Sun[1,3*], Wenmei Wang[1,3], Theresa Munyombwe[4] and Xuebin B. Yang[2,3,5*]

[1]Institute and Hospital of Stomatology, Nanjing University Medical School, Nanjing, 210008, PR China

[2]Biomaterials and Tissue Engineering Group, School of Dentistry, University of Leeds, Leeds LS2 9LU, UK.

[3]Nanjing-Leeds Joint Centre for Oral Health Science, No.30 Zhongyang Road, Nanjing, 210008, PR China

[4]Centre for Epidemiology & Biostatistics, University of Leeds, LS2 9LU, UK

[5]NIHR Leeds Musculoskeletal Biomedical Research Unit, Chapel Allenton Hospital, Leeds, LS7 4SA, UK.

Running title: Novel Mechanical loading model for hDPSCs osteogenesis

* Corresponding authors:

Dr Xuebin B Yang, Biomaterials and Tissue Engineering Group, School of Dentistry, University of Leeds, Leeds LS2 9LU, UK. E-mail: X.B.Yang@leeds.ac.uk.

Professor Weibin Sun, Institute and Hospital of Stomatology, Nanjing University Medical School, Nanjing, 210008, PR China. E-mail: wbsun@nju.edu.cn

Abstract

Tooth loss often results the alveolar bone resorption due to lack of mechanical stimulation. Thus, the mechanism of mechanical loading on stem cells osteogenesis is crucial for alveolar bone regeneration. This project aims to investigate the effect of mechanical loading on human dental pulp stromal cells (hDPSCs) osteogenesis in a novel in vitro model. Briefly, 1×10^7 hDPSCs were seeded into 1 mL 3% agarose gel in a 48-well-plate. Then a loading tube was placed in the middle of the gel to mimicking the tooth chewing movement (1Hz, 3×30 min per day. n=3). No loading group was used as control. At different time points, the distribution of live/dead cells within the gel was confirmed by fluorescent markers and confocal microscope. The correlation and interaction between the factors (e.g. force, time, depth, and distance) were statistically analyzed. The samples were processed for histology and immunohistochemistry.After 1- 3 weeks of culture in the in-house designed in vitro bioreactor, fluorescent imaging confirmed that additional mechanical loading increased the viable cell numbers along with time compared to control. Different phenotype cells formed different patterns away from the reaction tube. The cells in the middle part showed enhanced alkaline phosphatase staining at week 1 but reduced at weeks 2 & 3. Additional loading enhanced Sirius Red and Type I collagen staining compared to control. This study used a novel in-house designed biomimetic in vitro bioreactor mimicking biting force to enhance hDPSCs osteogenesis in agarose scaffold and promote bone formation and/or prevent bone resorption.

Keywords:biomimetic bioreactor; mechanical stimulation; biting force; hDPSCs; bone tissue engineering; osteogenesis; in vitro model

Abbreviation

ALP	alkaline phosphatase
CMFDA	5-chloromethylfluorescein diacetate
CO_2	carbon dioxide
DMSO	dimethylsulphoxide
EH-1	ethidium homodimer-1
FBS	fetal bovine serum
hDPSCs	human dental pulp stromal cells
P	Passage
P/S	penicillin and streptomycin

PBS	phosphate buffered saline
SD	standard deviations
α-MEM	Alpha-modified minimum essential medium

Introduction

It has been general accepted that chewing movement and the force created are very important for the maintenance of the shape and strength of the supporting alveolar bone, while loss of tooth always causes alveolar bone resorption due to lack of proper mechanical stimulation (Barros et al. 2007; Kingsmill 1999; Mavropoulos et al. 2007). This atrophy remodeling leads to morphology change, function loss, dental implant failure, etc (Tolstunov 2006). Current clinical therapies to alveolar bone loss are limited in using artificial bone substitutes and autogenic and allogenic bone grafts (Canter et al. 2007; Felix Lanao et al. 2012; Zietek et al. 2008). However, a number of limitations of using these conventional methods have led to the search for alternative approaches such as stem cell therapy and tissue engineering to tackle this clinical challenge (Green et al. 2004; Gu et al. 1997; Horner et al. 2010; Horner et al. 2008; Yang et al. 2004; Yang et al. 2003b).

It has been suggested that tissue engineering requires three basic elements: stem cell (key factor), growth factors, and extracellular scaffolds (Bruder and Fox 1999; Yang et al. 2003a).However, recent progress in this field has shown that the fourth element-mechanical stimulationis crucial for the quality and/or function of the regenerated tissue (Altman et al. 2002; Kimelman-Bleich et al. 2011; Terai et al. 1999; Yang et al. 2002).

Human dental pulp stromal cells (hDPSCs) were characterized as stem cells in 2000 (Alge et al. 2010; Gronthos et al. 2000). Thereafter, a number of studies confirmed that these cells are multi-potential and have the capacity to differentiate into progenitors which can

form bone, cartilage, adipose tissues, and so on (Laino et al. 2005; Min et al. 2008; Nakashima et al. 2009; Zhang et al. 2008).In recent years, it has been reported that mechanical loading could promote hDPSCs osteogenic differentiation and produce bone like tissue (Kraft et al. 2010; Kraft et al. 2011; Yu et al. 2009b). However, little consensus was achieved on the optimal mechanical parameters and the temporal sequence of applied mechanical loading (Sittichockechaiwut et al. 2009). Furthermore, it is very difficult to isolate the effect of a specific component of the physical milieu from the mechanical environment in all naturally observed or experimentally created conditions (Brown et al. 1990). In fact, Individual cells experience different combinations of substrate strain (e.g. tensile, compression, and shear); strain induced fluid flow depending on loading-related deformation of scaffold; and the hydrostatic compression from the environment (Burger et al. 1992; Hsieh and Turner 2001; van der Linden et al. 2001).The aim of this study was to mimic chewing force and to investigate the optimum mechanical force which could accelerate hDPSCs osteogenesis.

A bioreactor provides a controllable environment to create a bio-tissue both for systematic scientific research and for potential using in implant and replacement of damaged tissue (Sittichockechaiwut et al. 2009; Sittichokechaiwut et al. 2010).With regarding to mimicking the dynamics of the in vivo environment, the complexity of mechanical properties in different tissues (e.g. bone, cartilage, tendon and ligament, and cardiovascular tissue) should be considered and distinguished (Huselstein et al. 2008). In the case of bone tissue engineering, a few bioreactors existed for 3D-structure mechanical loading like mechanical

strains, bending, and fluid flow (Altman et al. 2002; Bancroft et al. 2002; Mauney et al. 2004). However, no previous published article was found related to specific designed bioreactor for alveolar bone. In an effort to fill this gap, an in-house mini-bioreactor has been developed so that dynamic physical stress from artificial tooth could be delivered into the alveolar bone shaped scaffold. Furthermore, this novel bioreactor is small enough to be cultured in the normal incubator, which facilitates the study of "chewing movement" on "alveolar bone tissue".

Material and Methods

Sample size

Sample size was bases on the primary objective of the study which was to compare the differences between loading and no loading groups at different time points. Sample size was determined in STATA version 11. Assuming a minimum difference of 50, power 90%, standard deviation from previous studies of 4, significances level 0.05 and two sided test, the study needed at least 3 samples per group.

Mechanism and design of loading device

Cyclic scaffold compression deformation at 1 Hz frequency has been general accepted as physiological loading simulations for the best mimic of chewing movement (Buschang et al. 2000; Huang et al. 2005; Pelaez et al. 2009; Terraciano et al. 2007). In this study, an

external 1 Hz frequency dynamic compressive force (Fig. 1) was applied to the loading groups 30 minutes each time and 3 times a day, no loading groups were used as negative control.

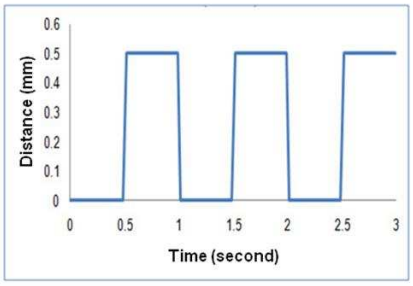

Fig.1 Rectangular wave form provided by external apparatus.

The apparatus was designed to model and analyze the force to cells in alveolar bone which endured strain and deformation during tooth chewing movement. It could be divided into two parts: loading component and cell culture part.

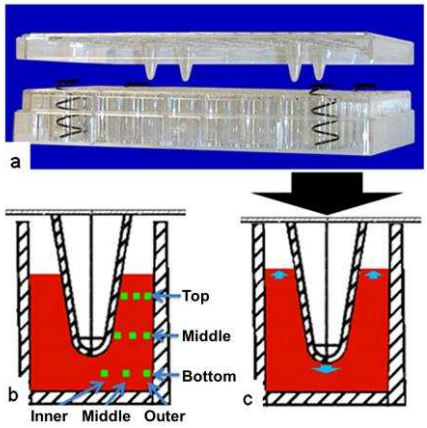

Fig. 2 Bioreactor housed in 48-well plate. a Four loading tubes were fixed on the lid. Four springs were positioned in the corners of the plate. b Schematic of an individual bioreactor with the gel casted in and chosen 9 squares (0.6 × 0.6 mm^2 each) for confocal observation. Factors related to space location in factorial analysis were depth at 3 levels (top, middle, and bottom), and distance at 3 levels (inner, middle, outer). c The 0.5 mm compressive displacement of the tube resulted in matrix elastic deformation with compression in the apex area and stretch in the top area.

The loading component (Fig. 2a) was used to pass the external pressure force to the cultured cells, which was comprised of two elements: loading body and displacement control. The loading body was trimmed top part (14 mm) of reaction tubes (0.5 mL Greiner Bio-One) symmetrical adhered firmly under the 48-well plate lid coaxial to the 4 wells below, passing

the movement directly to the cultured scaffold. The displacement control regulated tube maximum 0.5 mm vertical movement inside well through the fixed distance between the lid and plate, which could be adjusted by the length of 4 pieces of coiled spring placed in wells located in 4 corners of the plate. In the spring relaxed situation, 3 mm gap from the tube top end to the well bottom was pre-set. The parallel of rims between lid and plate guided the tube to the right ‘occlusion’.

The cell culture part (Fig. 2b) is located between the tube and well, which would be elaborated in the next paragraph.

Cells seeding and culture

Primary human dental pulp stromal cells (hDPSCs) were isolated from fresh extracted teeth from Leeds School of DentistryTissue Bank with ethical approval (three donors: two 8 and 12-year-old females, one 12-year-old male). The cells were in vitro expanded in culture medium containing alpha-modified minimum essential medium(α-MEM) supplemented with 10% fetal bovine serum (FBS), 100 U/mL penicillin, and 100 mg/L streptomycin (P/S) at 37ºC and 5% CO2. 1×10^7cells/mL hDPSCs (Passage 3: P3) were seeded into 3% agarose gel. Briefly, 3g agarose (Sigma A9045 Type VII low gelling temperature) was melted in warmed 100 mL 1 × phosphate buffered saline(PBS) (gel formation) and cooled down to 37°C. 5 mL melted gel was mixed with 5×10^7hDPSCs to yield 1×10^7 cells /mL gel and then the gel was aliquoted into the wells in the bioreactor described previously (1 mL per well, 4 wells per plate). Immediately (before the gel solidified/setting), the plate lid with four loading tubes

was place in position, the mixture was then cooled down to 20°C (the congealing temperature is 26-30°C), so that the cells seeded gel was cased around the loading tubes. After 6 hours, 200 µL culture media was added on top of the gel. These plates were cultured in a humidified incubator at 37°C and 5% CO_2. After 24 hours, cycling force was applied in loading groups. Culture media was changed every other day. At different time points (e.g. week1, 2, and 3), samples were labeled with fluorescent markers (see below) for confocal microscope observation or fixed in 98% ethanol overnight and embedded in paraffin block which were processed for histology.

Cell live/dead fluorescent labeling

50 µg Cell Tracker™ Green (5-chloromethylfluorescein diacetate: CMFDA, Molecular Probe), and an aliquot of ethidium homodimer-1 (EH-1) were dissolved in 10 µl dimethylsulphoxide (DMSO) and diluted in 5 mL serum-free α-MEM (final concentration: 20 µM CMFDA; 4 µM EH-1). After washed with 1 × PBS, the samples were put in 1 mL of this working solution and incubated at 37°C in darkness for 45 minutes. Then, the working solution was replaced with fresh pre-warmed α-MEM. After further 30 minutes incubating, the samples were washed again and assessed with confocal microscope.

Visualization of cell morphology, viability and density using confocal microscope

Cell viability within the gel was visualized under confocal laser scanning microscope (Leica TCS SP2)with Argon 488nm and He/Ne 543 nm laser sources, detection wavelengths

were within band 506~538 nm(green), and band 590~ 703 nm(red).

Nine 0.6×0.6mm^2 at different locations of the central longitudinal section of agarose gel were identified for observation (Fig. 2b). They represented different combinations of 3 levels of substrate strain according to the distance to the loading tube (inner zone - 1/3 which is close to the tube; middle zone - the mid 1/3; and outer zone -1/3 which is close to the wall of culture plate well) and 3 levels of hydrostatic compression by the depth (top part - top 1/3 of the gel; middle part - the mid part of the gel; and bottom part - the bottom 1/3 of the gel). 110 series sections (1.5 μm per section, total 165 μm thick) at 10× objectives were collected as Z-series sections and projected onto one plane as accumulated maximum for quantitative measurement of cell density. Live cell numbers were correlated to the green area, whereas dead cell numbers were correlated to the red area. Fluorescent intensity of the live/dead stain was quantitatively analyzed with Leica Confocal Software (version 2.61), by which the area of green and red were calculated respectively.

Alkaline phosphatase (ALP) staining

The sections were incubated with Sigma-Aldrich Alkaline Phosphatase kits (Fast Violet B Salt, Naphthol AS-MX Phosphate Alkaline Solution) at room temperature for 30 min using our well developed protocol (Green, Howard et al. 2003). Red color indicated positive staining for ALP.

Alcian blue/Sirius red staining

The sections were stained with Weigerthematoxylin solutions for 10 min (nuclear staining), which was followed by 20 min staining in 0.5% Alcian blue. Then the sections were treated with 1% molybdophosphoric acid for 20 min prior to be stained with 0.1% Sirius red for 1 h (collagen matrix) (Jones and Yang 2011).

Immunohistochemistry staining for type I collagen

The antigens were retrieved using Vector solution in pressure cooker. Then sections were blocked with normal goat serum, stained with type I collagen primary antibody (mouse monoclonal anti-collagen I from Abcam, ab6308) at 1:100 dilution overnight. After applied EnVision solution A, sections were developed in EnVision DAB for 5 min. Finally, sections were counterstained in Harris's Haematoxylin (30 sec). In negative controls, primary antibody incubation step was omitted.

Statistical Analysis

Cell density data were analyzed using PASW Statistics 18. Descriptive statistics such as means and standard deviations (SD) were used to summarize quantitative data. Box plots were used to compare groups. Since the treatment structure is factorial, a factorial analysis approach was adopted with 4 factors , namely: force at 2 levels (loading and no loading), time at 3 levels (1 week, 2 weeks, and 3 weeks), depth at 3 levels (top, middle, and bottom parts) , and distance at 3 levels (inner, middle, and outer zones).

Fixed effect factorial ANOVA was used to compare the main effects and interaction of loading, distance, time and depth. Normal probability plots were used to check whether the residuals were normally distributed. A square root transformation was conducted to normalize the residuals. The homogeneity of variance assumption was checked using a plot of residuals against fitted values. Tukey's Multiple Comparison Test was used to identify pairs that were significantly different, with the Tukey's Test adjusting for multiple comparisons. P value less than 0.05 was considered significant.

Results

Effect of loading to cell morphology

Different hDPSCs patterns in longitudinal section were observed both in confocal image and histology stained slices (Fig. 3).

Brightened live hDPSCs clusters with a range of size of 20-60μm in diameter (the average observed individual hDPSC size is 10μm) were

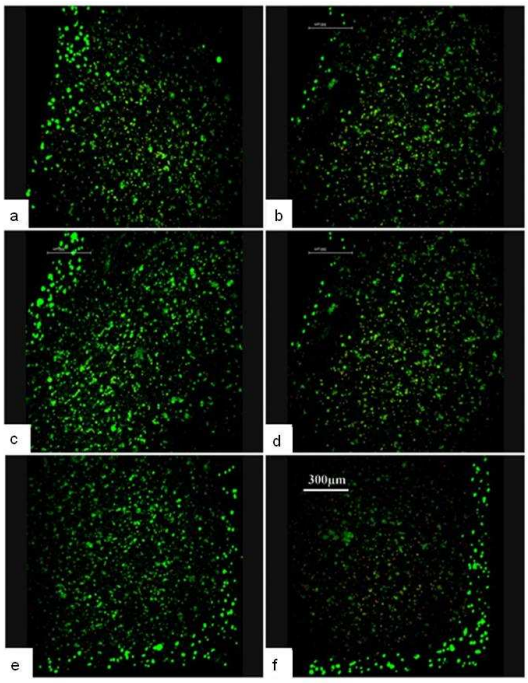

Fig. 3 Cell viability, morphology, density, distribution and alignment in the gel. After live (green) and dead (red) fluorescent labeling, hDPSCs observed by confocal microscope in mechanical loading group (a, c, e) in different depth at week 1 compared with static controls (b, d, f). a & b the top parts with tube on the left, c & d the middle parts with tube on the left, e & f the bottom parts with wall of well on the right. Scale bars: 300 μm.

notable in the band near the loading tube. In comparison, they were rare to be seen in middle zone. However, in the outer zone where close to the wall of well, the cell cluster band could be noticed again. The band width per group was obtained by the average value of measurements at 3 locations in 3 samples, which varied with time respectively in loading group and no loading control. In loading group, at week 1, the widths reached 300μm (near the tube) and 150μm (near the wall); at week 2 and 3, this kind of edge effect faded down along with culture time perhaps due to the increase of cell numbers inside the gel. In contrast, in no loading control, at week 1, the widths were 150μm in the inner zone and 120μm in the outer zone; and thinner stripes of clusters still maintained in the following 2 weeks.

In respect to hDPSCs arrangement, it could be seen that the loading seemly enhanced cell alignment complying with matrix deformation in longitudinal section in loading group, which was different according to the depth in gel. In the bottom area, cells were ordered from apex of the tube towards surface of the well bottom. In the middle part, an outward and upward cell arrangement was observed. In the top zone, cells appeared parallel to the outside surface of the loading tube.

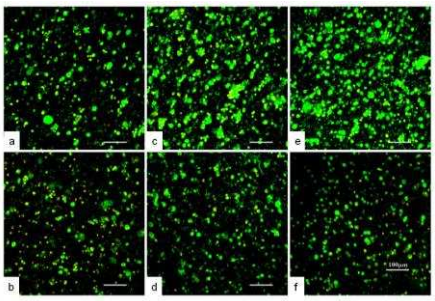

Fig. 4 The comparison of cell density and alignment between two groups at different time points. Live (green) and dead (red) fluorescent labeling and confocal microscope showed that enhanced cell density and alignment observed in mechanical loading group along at week 1, 2, and 3 (a, c, e) compared with static controls (b, d, f). Scale bars: 100 μm.

Effect of loading to cell proliferation

The different distribution of hDPSCs

proliferation in longitudinal section was reflected by the CMFDA fluorescent marker in confocal image (Fig. 4), which was supported by the histology observation.

The density of live cells was influence by three elements: depth, distance, and interaction of force (loading and no loading) and time. 1) With regards to the depth (Fig. 5a), the middle part of the gel appeared to have the highest density, which was followed by the bottom part (9.8% less than the middle part, but P>0.05). The density in the top part was the lowest, about 40% less than that in the middle (P<0.001); 2) with respect to the distance (Fig. 5c), the density of live cells reduced along with the increase of distance from the loading tube. The outer zone shared the lowest live cell density, which was about 40% less than that in the inner zone (P<0.001).While, there was no significant difference between the density in the middle zone and the inner zone, though the former was

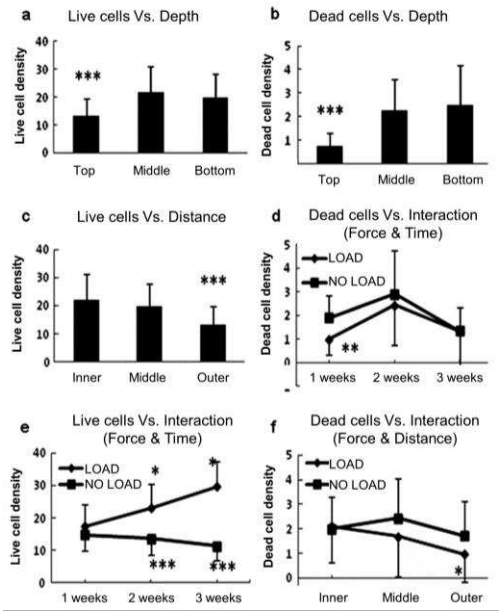

Fig. 5 The comparison of live and dead cells in nine chosen areas at week 1, 2 and 3 (Mean ± SD; n=3). a Live cells versus depth in gel (top upper 1/3, middle intermediate 1/3, and bottom lower 1/3), b Dead cells versus depth in gel, c Live cells versus distance from the loading tube (inner zone near 1/3, middle zone intermediate 1/3, and outer zone far 1/3), d Interaction of force and time (e.g. 1, 2, and 3 weeks) on live cells, e Interaction of force and time (e.g. 1, 2, and 3 weeks) on dead cells, f Interaction of force and distance on dead cells. Keys for statistic comparison: *** P<0.001; ** P<0.01; * P<0.05. Keys for statistic analysis: a~c difference from other two groups, d) difference from previous time point in loading group, e Top: loading group is different from no loading control at 1 week, Bottom: difference from no load control at same time point, f the outer zone is different from the inner zone in loading group.

10% less than the latter; 3) In terms of force (loading and no loading), it was time dependent (Fig. 5e). In loading group, the density of live cells was enhanced gradually. Meanwhile, the weekly increase of the density (approximately 30%) in loading group was significant ($P<0.05$). In contrast, in the no loading group, the density fell steadily however with no significant difference. When it was compared between loading and no loading groups, there was no statistically significant difference at 1 week. However, at 2 weeks, the density in loading group was about 60% higher than that in the no loading group ($P<0.001$). By 3 weeks, the cell density in loading group was nearly 3 times compared to that in no loading control ($P<0.001$).

Effect of loading to cell death

The distribution of dead cells in the same area as live cellswas also investigated.

The density of dead cells was also related to three determinants: depth, combination of force and time, joint of force and distance. 1) Concerning the depth (Fig. 5b): the dead cell density showed an upward trend with the increase of the depth. The top part approached the minimum, which was only one third of that in the middle ($P<0.001$). Towards the bottom part, the dead cell density reached the peak density (11.2% higher than that in the middle, but $P>0.05$); 2) In regarding to the force (loading and no loading), it was also time dependent (Fig. 5d): Although loading could reduce the dead cells density in each time point, only at 1 week, there was a significant decrease (50%) in dead cell density in the loading group compare to that in no loading groups ($P<0.01$); 3) With respect to the interaction of distance

and force (loading and no loading) (Fig. 5f): In the loading group, the dead cells declined steadily from the inner zone (close to the loading tube) to the outer zone (close to the wall). Density in the outer zone dropped down more than 50% compared to that in the inner zone ($P<0.05$). Nevertheless, in no loading group, there was no statistic difference among three levels in distance.

Effect of loading to cell osteogenic differentiation

As one of the osteogenic early markers, ALP staining was used to detect whether hDPSCs still maintained the ability of osteogenesis. At week 1, ALP expression of hDPSCs became most intensive (Fig. 6a, 6b). However, the ALP stain was slightly lighter at week 2 and 3. There was more positive ALP staining in the loading group compared to no loading control although this was not a quantitative assay (Fig. 6c-f).

Alcian blue/Sirius red stained (Fig. 7a, 7b, 7c, 7d) showed that some blue stained individual cells appeared in the top area in the loading group and the numbers were increased along with time. In contrast, there was no blue staining in the no loading group. On the other hand, many Sirius red stained hDPSCs clusters were found mainly in middle and bottom areas at week 1 in both

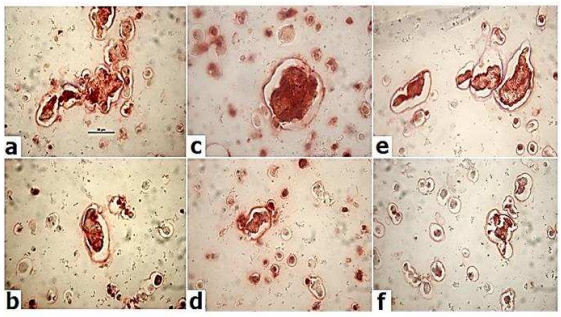

Fig. 6 The comparison of intensity of ALP staining between loading groups (a, c, e) and no loading controls (b, d, f). a & b week 1; c & d week 2; e & f week 3. Load groups seemed to have more positive staining than static controls. Stain at week 2 and 3 is slight weaker than that at week 1. Scale bar: 50μm.

loading and no loading groups. In loading group, the amount of such clusters enhanced over the time. On the contrary, the cluster numbers decreased steadily in the no loading control.

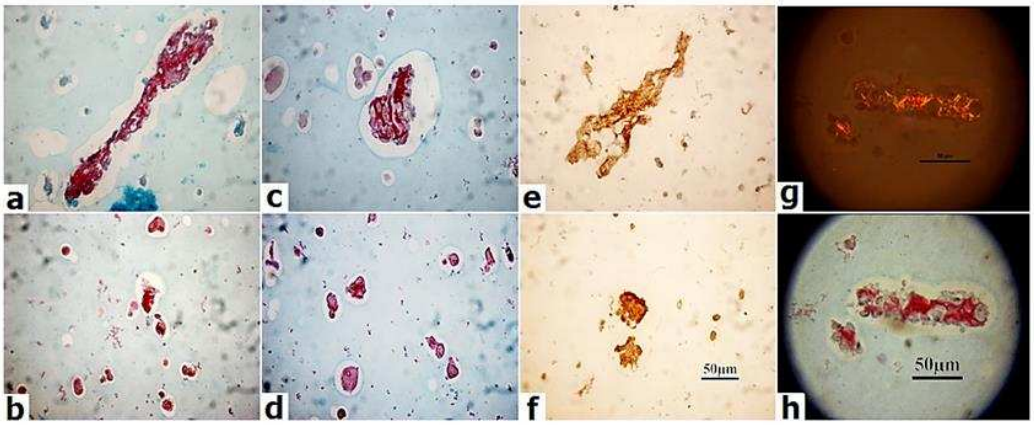

Fig. 7 Histological analysis showed cell osteogenic differentiation, extracellular matrix deposition in the gel. Mechanical loading group (a, c, e, g, h) compared with static controls (b, d, f) at week 1. a & b Alcian blue/Sirius red staining in middle zone. c & d Alcian blue/Sirius red staining in outer zone, e & f Type I collagen immunohistochemical staining. g Birefringence image showed type I collagen matrix formation within the mechanical loading group, h Alcian blue/Sirius red staining for the same section as figure 7g. Scale bars: 50 μm.

In addition, in terms of the shape of the cluster, it seemed that more clusters lined up to the matrix deformation in loading group, which was similar to that mentioned previously, compared to that in the no loading control. Collagen pattern inside the cell cluster were different among groups and these were also confirmed by the strong brown stain of type I collagen immunohistochemistry (Fig. 7e, 7f). On the other hand, the anisotropic arrangement of collagen fibers along the ridge of cell clusters displayed a distinct birefringence when viewed by polarized light (Fig. 7g), and these were similar to the Alcian blue/Sirius red staining in a parallel session (Fig. 7h).

Discussion

Bioreactor design and loading application

Previous studies on human chewing cycle showed that average chewing frequency was about 1 Hz (Buschang et al. 2000). To achieve this, a dynamic compressive force (30 minutes each time and 3 times a day) was applied to the loading groups; no loading groups were used as negative control.

A number of studies have shown that 5-10% tension can be used to promote viability, proliferation and osteogenesis of hDPSCs(Yu et al. 2009a). 5% global strain of compression was applied for bone formation (Sittichockechaiwut et al. 2009; Sittichokechaiwut et al. 2010). Although, it was proved mechanical stimulation affected the cell behavior in the construct as a whole, few researches looked into a scaffold to find the differences among areas except for some computer models (Lacroix et al. 2006; O'Brien et al. 2007). In the present study, dynamic mechanical strains were applied to hDPSCs-agarose gel matrix in a half restrict space. Comparisons of cell behavior were done among different areas in a longitudinal section. The 0.5 mm compressive displacement of the tube resulted in matrix elastic deformation (Fig. 2c), which was a combination of dynamic compression and stretch, varying along with different locations in the matrix. Due to the constancy of overall gel volume, approximately 16% compression (maximum 0.5 mm) took place in the apex (center bottom) area, while about 6% of stretch (maximum 0.6mm) appeared in the top area. However, most part of the matrix in the middle area had a deformation within this range.

Scaffold choosing

Three dimensional agarose gel scaffold have been used to long term culture and study cell phenotype expression, proliferation, and differentiation for a long time (Benya and Shaffer 1982; Kolettas et al. 1995; Kurane and Vyavahare 2009; Mouw et al. 2005). A number of recent studies used agarose gel to investigate cells behavior under different kinds of dynamic mechanical loading (Altman et al. 2002; Buschmann et al. 1995; Knight et al. 1998; Winer et al. 2009).

In this study, agarose gel was chose as a supportive material to investigate mechanical loading to hDPSCs based on two aspects. For one thing, its uniform, simplicity, reproducibility, and capacity to apply physiological level strain proved a suitable environment for investigation of mechanical loading. For another, it polymerized to a three dimensional structure with adjustable strength with open lattice, minimizing diffusion distances as well as fixing cells, which may be useful for creating an artificial tissue for clinical restoration. Researches on choosing of agarose gel concentration illustrated that the pore diameter increased when the agarose concentration declined and vise verse the wide pore diameter distribution narrowed as the gel concentration enhanced (Maaloum et al. 1998). The hydraulic permeability of 3% agarose gel was $36.9 \pm 4.6 \times 10^{-15}\ m^4/(N.s)$ (Buschmann et al. 1995), while it was $51.4 \pm 8.5 \times 10^{-15}\ m^4/(N.s)$ for 2% agarose gel (Buschmann et al. 1992). With cells cased, the permeability was lower than the gel without cells at the initial stage and further decreased along the culture for cell matrix deposit. However, with regard to the

rigidity of scaffold, it has been suggested that stem cells become osteoblasts-like when cultured on stiff matrix (34 kPa hydrogels), while they become neuron-like, myocyte-like on soft ones (Reilly and Engler 2010). Thus, higher concentration of agarose gel (more rigid) with reasonable hydraulic permeability (nutrition and waste exchange) may be better to create similar microenvironment in vitro for bone tissue regeneration. Different concentrations of agarose gel were compared in our pre-study and 3% concentration was selected by balancing the suitable rigidity for long-time loading and good permeability facilitating the nutrition exchange.

There were no obvious cracks, fracture and plastic deformation in the agarose gel through 3 weeks of loading. However, accumulated small cracks and breaks were detected in the gel after 4 weeks no matter in loading or no loading groups. The gel scaffold is planned to be reinforced by some ingredient in expecting the integrity would be preserved longer in the future study.

Cell behavior various in different area and time

HDPSCs behavior changes inside the matrix were relevant to the deformation of the surrounding gel. As a whole, in accordance with the results of previous researches, mechanical stimulation could enhance hDPSCs viability and proliferation along with time compare to the no loading control. Furthermore, there was improved cell alignment to the

matrix deformation in the longitudinal section. The phenomenon is assumed that force plays an important role in regulating cellular polarity during mitosis. In addition, collagen matrix stained by Sirius red concentrated in the middle and bottom area, while proteoglycans dyed by Alcian blue focused in the top part. That change may indicate that pressure contribute to cell proliferation and osteogenesis, tensile probably inhibited cell proliferation and enhance chondrogenesis.

Concerning the dead cell distribution pattern, it is different to that of live cells. The dead cell number was significantly decreased at week 1 by mechanical loading, but the difference disappeared in week 2 & 3, which may implied that cell translation of mechanical signals changed when hDPSCs were in different differentiation stage (Weyts et al. 2003). Based on our in vitro model, the deformation of the gel matrix in the outer zone was less than that near the tube, it is interesting to note that loading only decreased dead cell numbers in the outer zone while enhanced live cell numbers more in the inner zone. We suspected if cells needed different kind of mechanical environment between just kept viability (low force) and proliferation (high force). Or perhaps the reason may only be relate to the numbers of live cells, which decreased with the increase of the distance for the tube.

In terms of less live and dead cell density in the top part of the gel matrix, we could not explain that very clear for hDPSCs were evenly mixed into agarose gel prior to casting. We do not know if gravity played a role in that phenomenon.

With regard to the time played in cell differentiation, comparison was done based on

histological staining. ALP activity, as an early marker of osteoblastic phenotype, peaked at week 1, and still existed at week 2 & 3, both in loading and no loading groups. By comparison, extracellular matrix formation and composition differed between loading and no loading groups with time. These may suggest that hDPSCs maintain the ability of osteogenesis well in the present 3% agarose gel culture system. Meanwhile, loading seems have the ability to promote the osteogenic potential to the real bone like matrix formation.

In relate to the observed brightened live hDPSCs gobbets in the band near the reaction tube and wall of well, we have not found any similar description in the publications. On the one hand, since it is a semi-restrict system, the wedge effect happened when the tube was pressed down, the dynamic substrate shear stress occurred in the part of gel near tube. Not only the shear stress could cause augment of cell osteogenesis (Grellier et al. 2009; Jacobs et al. 1998; Liu et al. 2012), but also the induced fluid flow may enhance the streaming potential and nutrients transport to the inner zone, which were assumed to contribute to cell aggregation. The phenomenon that more cell matrix biosynthesis was detected in outer ring compared to the center when dynamic mechanical compression was applied to three dimension scaffold in vitro was found in previous researches (Buschmann et al. 1995; Kim et al. 1994; Sittichockechaiwut et al. 2009), which may partly explain the fluid flow effect. On the other hand, as to the agglomerate cell stripe near the wall of well, we hypothesize that it had something to do with the seep down of media through the micro gap between gel and well.

Conclusion

The in-house designed in vitro bioreactor mimics the biting force which can be useful in investigating the effect of complex mechanical stimulation to bone formation. The enhanced hDPSCsosteogenesis may shed a light on promoting new bone formation and preventing bone resorption for translational clinical therapy in both orthopaedics and dentistry.

Acknowledgements

J.J. was funded by the Jiangsu Government Scholarship for Overseas Studies, PR China; Natural Science Foundation of Jiangsu Province (No.BK20130081), and Jiangsu Province's Outstanding Medical Academic Leader program (No.LJ201110). We thank Dr. Raif & Mr. Pullan for assistance on the manufacture of the bioreactor. This project was partially funded by the Royal Society International Exchanges Award, World Universities Network (WUN) and National Institute for Health Research (NIHR). The research leading to these results has received funding from the European Union Seventh Framework Programme ([FP7/2007-2013] [FP7/2007-2011]) under grant agreement n° [318553].

References

Alge DL, Zhou D, Adams LL, Wyss BK, Shadday MD, Woods EJ, Gabriel Chu TM, Goebel WS (2010) Donor-matched comparison of dental pulp stem cells and bone marrow-derived mesenchymal stem cells in a rat model. Journal of tissue engineering and regenerative medicine 4:73-81

Altman GH, Horan RL, Martin I, Farhadi J, Stark PR, Volloch V, Richmond JC, Vunjak-Novakovic G, Kaplan DL (2002) Cell differentiation by mechanical stress. FASEB J 16:270-272

Bancroft GN, Sikavitsas VI, van den Dolder J, Sheffield TL, Ambrose CG, Jansen JA, Mikos AG (2002) Fluid flow increases mineralized matrix deposition in 3D perfusion culture of marrow stromal osteoblasts in a dose-dependent manner. Proceedings of the National Academy of Sciences of the United States of America 99:12600-12605

Barros I, Muramoto T, Soma K (2007) Effects of occlusal loading on alveolar bone remodeling and changes in the distribution of neuropeptides after tooth replantation in rats. J Med Dent Sci 54:49-56

Benya PD, Shaffer JD (1982) Dedifferentiated chondrocytes reexpress the differentiated collagen phenotype when cultured in agarose gels. Cell 30:215-224

Brown TD, Pedersen DR, Gray ML, Brand RA, Rubin CT (1990) Toward an identification of mechanical parameters initiating periosteal remodeling: a combined experimental and analytic approach. J Biomech 23:893-905

Bruder SP, Fox BS (1999) Tissue engineering of bone. Cell based strategies. Clin Orthop Relat Res S68-83

Burger EH, Klein-Nulend J, Veldhuijzen JP (1992) Mechanical stress and osteogenesis in vitro. J Bone Miner Res 7 Suppl 2:S397-401

Buschang PH, Hayasaki H, Throckmorton GS (2000) Quantification of human chewing-cycle kinematics. Arch Oral Biol 45:461-474

Buschmann MD, Gluzband YA, Grodzinsky AJ, Hunziker EB (1995) Mechanical compression modulates matrix biosynthesis in chondrocyte/agarose culture. J Cell Sci 108 (Pt 4):1497-1508

Buschmann MD, Gluzband YA, Grodzinsky AJ, Kimura JH, Hunziker EB (1992) Chondrocytes in agarose culture synthesize a mechanically functional extracellular matrix. Journal of orthopaedic research : official publication of the Orthopaedic Research Society 10:745-758

Canter HI, Vargel I, Mavili ME (2007) Reconstruction of mandibular defects using autografts combined with demineralized bone matrix and cancellous allograft. J Craniofac Surg 18:95-100; discussion 101-103

Felix Lanao RP, Hoekstra JW, Wolke JG, Leeuwenburgh SC, Plachokova AS, Boerman OC, van den Beucken JJ, Jansen JA (2012) Porous calcium phosphate cement for alveolar bone regeneration. J Tissue Eng Regen

Med

Green D, Walsh D, Yang XB, Mann S, Oreffo ROC (2004) Stimulation of human bone marrow stromal cells using growth factor encapsulated calcium carbonate porous microspheres. J Mater Chem 14:2206-2212

Grellier M, Bareille R, Bourget C, Amedee J (2009) Responsiveness of human bone marrow stromal cells to shear stress. J Tissue Eng Regen Med 3:302-309

Gronthos S, Mankani M, Brahim J, Robey PG, Shi S (2000) Postnatal human dental pulp stem cells (DPSCs) in vitro and in vivo. Proc Natl Acad Sci U S A 97:13625-13630

Gu YD, Cheng DS, Zhang GM, Chen XM, Xu JG, Yang XB (1997) Long-term results of toe transfer: retrospective analysis. J Reconstr Microsurg 13:405-408

Horner E, Kirkham J, Wood D, Curran S, Smith M, Thomson B, Yang X (2010) Long Bone Defect Models for Tissue Engineering Applications: Criteria for Choice. Tissue Engineering Part B 16:263-271

Horner E, Kirkham J, Yang X (2008) Animal Models In: Polak JM, S; Harding,SE (ed) Advances in tissue engineering. Imperial College Press, London, pp 763-780

Hsieh YF, Turner CH (2001) Effects of loading frequency on mechanically induced bone formation. J Bone Miner Res 16:918-924

Huang CY, Reuben PM, Cheung HS (2005) Temporal expression patterns and corresponding protein inductions of early responsive genes in rabbit bone marrow-derived mesenchymal stem cells under cyclic compressive loading. Stem Cells 23:1113-1121

Huselstein C, Netter P, de Isla N, Wang Y, Gillet P, Decot V, Muller S, Bensoussan D, Stoltz JF (2008) Mechanobiology, chondrocyte and cartilage. Biomed Mater Eng 18:213-220

Jacobs CR, Yellowley CE, Davis BR, Zhou Z, Cimbala JM, Donahue HJ (1998) Differential effect of steady versus oscillating flow on bone cells. J Biomech 31:969-976

Jones E, Yang X (2011) Mesenchymal stem cells and bone regeneration: Current status. Injury 42:562-568

Kim YJ, Sah RL, Grodzinsky AJ, Plaas AH, Sandy JD (1994) Mechanical regulation of cartilage biosynthetic behavior: physical stimuli. Arch Biochem Biophys 311:1-12

Kimelman-Bleich N, Seliktar D, Kallai I, Helm GA, Gazit Z, Gazit D, Pelled G (2011) The effect of ex vivo dynamic loading on the osteogenic differentiation of genetically engineered mesenchymal stem cell model. J Tissue Eng Regen Med 5:384-393

Kingsmill VJ (1999) Post-extraction remodeling of the adult mandible. Crit Rev Oral Biol Med 10:384-404

Knight MM, Lee DA, Bader DL (1998) The influence of elaborated pericellular matrix on the deformation of isolated articular chondrocytes cultured in agarose. Biochim Biophys Acta 1405:67-77

Kolettas E, Buluwela L, Bayliss MT, Muir HI (1995) Expression of cartilage-specific molecules is retained on long-term culture of human articular chondrocytes. J Cell Sci 108 (Pt 5):1991-1999

Kraft DC, Bindslev DA, Melsen B, Abdallah BM, Kassem M, Klein-Nulend J (2010) Mechanosensitivity of dental pulp stem cells is related to their osteogenic maturity. Eur J Oral Sci 118:29-38

Kraft DC, Bindslev DA, Melsen B, Klein-Nulend J (2011) Human dental pulp cells exhibit bone cell-like responsiveness to fluid shear stress. Cytotherapy 13:214-226

Kurane A, Vyavahare N (2009) In vivo vascular tissue engineering: influence of cytokine and implant location on tissue specific cellular recruitment. J Tissue Eng Regen Med 3:280-289

Lacroix D, Chateau A, Ginebra MP, Planell JA (2006) Micro-finite element models of bone tissue-engineering scaffolds. Biomaterials 27:5326-5334

Laino G, d'Aquino R, Graziano A, Lanza V, Carinci F, Naro F, Pirozzi G, Papaccio G (2005) A new population of human adult dental pulp stem cells: a useful source of living autologous fibrous bone tissue (LAB). J Bone Miner Res 20:1394-1402

Liu L, Zong C, Li B, Shen D, Tang Z, Chen J, Zheng Q, Tong X, Gao C, Wang J (2012) The interaction between beta1 integrins and ERK1/2 in osteogenic differentiation of human mesenchymal stem cells under fluid shear stress modelled by a perfusion system. J Tissue Eng Regen Med

Maaloum M, Pernodet N, Tinland B (1998) Agarose gel structure using atomic force microscopy: gel concentration and ionic strength effects. Electrophoresis 19:1606-1610

Mauney JR, Sjostorm S, Blumberg J, Horan R, O'Leary JP, Vunjak-Novakovic G, Volloch V, Kaplan DL (2004) Mechanical stimulation promotes osteogenic differentiation of human bone marrow stromal cells on 3-D partially demineralized bone scaffolds in vitro. Calcified tissue international 74:458-468

Mavropoulos A, Rizzoli R, Ammann P (2007) Different responsiveness of alveolar and tibial bone to bone loss stimuli. J Bone Miner Res 22:403-410

Min KS, Park HJ, Lee SK, Park SH, Hong CU, Kim HW, Lee HH, Kim EC (2008) Effect of mineral trioxide aggregate on dentin bridge formation and expression of dentin sialoprotein and heme oxygenase-1 in human dental pulp. J Endod 34:666-670

Mouw JK, Case ND, Guldberg RE, Plaas AH, Levenston ME (2005) Variations in matrix composition and GAG fine structure among scaffolds for cartilage tissue engineering. Osteoarthritis Cartilage 13:828-836

Nakashima M, Iohara K, Sugiyama M (2009) Human dental pulp stem cells with highly angiogenic and neurogenic potential for possible use in pulp regeneration. Cytokine Growth Factor Rev 20:435-440

O'Brien FJ, Harley BA, Waller MA, Yannas IV, Gibson LJ, Prendergast PJ (2007) The effect of pore size on permeability and cell attachment in collagen scaffolds for tissue engineering. Technol Health Care

15:3-17

Pelaez D, Huang CY, Cheung HS (2009) Cyclic compression maintains viability and induces chondrogenesis of human mesenchymal stem cells in fibrin gel scaffolds. Stem Cells Dev 18:93-102

Reilly GC, Engler AJ (2010) Intrinsic extracellular matrix properties regulate stem cell differentiation. Journal of biomechanics 43:55-62

Sittichockechaiwut A, Scutt AM, Ryan AJ, Bonewald LF, Reilly GC (2009) Use of rapidly mineralising osteoblasts and short periods of mechanical loading to accelerate matrix maturation in 3D scaffolds. Bone 44:822-829

Sittichokechaiwut A, Edwards JH, Scutt AM, Reilly GC (2010) Short bouts of mechanical loading are as effective as dexamethasone at inducing matrix production by human bone marrow mesenchymal stem cell. Eur Cell Mater 20:45-57

Terai K, Takano-Yamamoto T, Ohba Y, Hiura K, Sugimoto M, Sato M, Kawahata H, Inaguma N, Kitamura Y, Nomura S (1999) Role of osteopontin in bone remodeling caused by mechanical stress. J Bone Miner Res 14:839-849

Terraciano V, Hwang N, Moroni L, Park HB, Zhang Z, Mizrahi J, Seliktar D, Elisseeff J (2007) Differential response of adult and embryonic mesenchymal progenitor cells to mechanical compression in hydrogels. Stem Cells 25:2730-2738

Tolstunov L (2006) Dental implant success-failure analysis: a concept of implant vulnerability. Implant Dent 15:341-346

van der Linden JC, Homminga J, Verhaar JA, Weinans H (2001) Mechanical consequences of bone loss in cancellous bone. J Bone Miner Res 16:457-465

Weyts FA, Bosmans B, Niesing R, van Leeuwen JP, Weinans H (2003) Mechanical control of human osteoblast apoptosis and proliferation in relation to differentiation. Calcif Tissue Int 72:505-512

Winer JP, Janmey PA, McCormick ME, Funaki M (2009) Bone marrow-derived human mesenchymal stem cells become quiescent on soft substrates but remain responsive to chemical or mechanical stimuli. Tissue Eng Part A 15:147-154

Yang X, Tare RS, Partridge KA, Roach HI, Clarke NM, Howdle SM, Shakesheff KM, Oreffo RO (2003a) Induction of human osteoprogenitor chemotaxis, proliferation, differentiation, and bone formation by osteoblast stimulating factor-1/pleiotrophin: osteoconductive biomimetic scaffolds for tissue engineering. J Bone Miner Res 18:47-57

Yang XB, Bhatnagar RS, Li S, Oreffo RO (2004) Biomimetic collagen scaffolds for human bone cell growth and differentiation. Tissue Eng 10:1148-1159

Yang XB, Green DW, Roach HI, Clarke NM, Anderson HC, Howdle SM, Shakesheff KM, Oreffo RO (2003b) Novel osteoinductive biomimetic scaffolds stimulate human osteoprogenitor activity--implications for skeletal repair. Connect Tissue Res 44 Suppl 1:312-317

Yang Y, Magnay JL, Cooling L, El HA (2002) Development of a 'mechano-active' scaffold for tissue engineering. Biomaterials 23:2119-2126

Yu J, Xie YJ, Xu D, Zhao SL (2009a) [Effect of cyclic strain on cell morphology, viability and proliferation of human dental pulp cells in vitro]. Shanghai Kou Qiang Yi Xue 18:599-603

Yu V, Damek-Poprawa M, Nicoll SB, Akintoye SO (2009b) Dynamic hydrostatic pressure promotes differentiation of human dental pulp stem cells. Biochem Biophys Res Commun 386:661-665

Zhang W, Walboomers XF, Van Kuppevelt TH, Daamen WF, Van Damme PA, Bian Z, Jansen JA (2008) In vivo evaluation of human dental pulp stem cells differentiated towards multiple lineages. J Tissue Eng Regen Med 2:117-125

Zietek M, Gedrange T, Mikulewicz M (2008) Long term evaluation of biomaterial application in surgical treatment of periodontosis. J Physiol Pharmacol 59 Suppl 5:81-86